American Journal of Pathology, Vol. 167, No. 2, August 2005

Neurobiology

Cerebral Microvascular Amyloid β Protein Deposition Induces Vascular Degeneration and Neuroinflammation in Transgenic Mice Expressing Human Vasculotropic Mutant Amyloid β Precursor Protein

Jianting Miao,* Feng Xu,* Judianne Davis,* Irene Otte-Höller,† Marcel M. Verbeek,‡ and William E. Van Nostrand*

From the Department of Medicine, Health Sciences Center, Stony Brook University, Stony Brook, New York; and the Departments of Pathology† and Neurology,‡ Radboud University Nijmegen Medical Centre, Nijmegen, The Netherlands*

Cerebral vascular amyloid β-protein (Aβ) deposition, also known as cerebral amyloid angiopathy, is a common pathological feature of Alzheimer's disease. Additionally, several familial forms of cerebral amyloid angiopathy exist including the Dutch (E22Q) and Iowa (D23N) mutations of Aβ. Increasing evidence has associated cerebral microvascular amyloid deposition with neuroinflammation and dementia in these disorders. We recently established a transgenic mouse model (Tg-SwDI) that expresses human vasculotropic Dutch/Iowa mutant amyloid β-protein precursor in brain. Tg-SwDI mice were shown to develop early-onset deposition of Aβ exhibiting high association with cerebral microvessels. Here we present quantitative temporal analysis showing robust and progressive accumulation of cerebral microvascular fibrillar Aβ accompanied by decreased cerebral vascular densities, the presence of apoptotic cerebral vascular cells, and cerebral vascular cell loss in Tg-SwDI mice. Abundant neuroinflammatory reactive astrocytes and activated microglia strongly associated with the cerebral microvascular fibrillar Aβ deposits. In addition, Tg-SwDI mouse brain exhibited elevated levels of the inflammatory cytokines interleukin-1β and -6. Together, these studies identify the Tg-SwDI mouse as a unique model to investigate selective accumulation of cerebral microvascular amyloid and the associated neuroinflammation. *(Am J Pathol 2005, 167:505–515)*

The progressive cerebral accumulation of amyloid β-protein (Aβ) in parenchymal senile plaques and in the cerebral vasculature is a primary pathological feature of Alzheimer's disease (AD) and several related disorders.[1–3] The Aβ peptide is derived from the Aβ precursor protein (AβPP), a type I integral membrane protein, through sequential proteolytic processing mediated by β- and γ-secretase activities.[1,4] Several mutations in the AβPP gene have been identified that reside within mid-region residues of Aβ, including the Dutch E22Q and Iowa D23N variants, which result in familial forms of early-onset and severe cerebral amyloid angiopathy (CAA).[5–9] Recent studies have suggested that cerebral microvascular amyloid accumulation is a better correlate with dementia than parenchymal amyloid plaques.[10,11] Moreover, cerebral microvascular amyloid, especially in familial CAA disorders, is associated with a localized neuroinflammatory reaction.[9,12–17] Together, these findings underscore the increasing recognition of the importance of cerebral microvascular amyloid-induced neuroinflammation and dementia.

Recently, we generated transgenic mice (Tg-SwDI) that express human Swedish/Dutch/Iowa mutant AβPP in brain.[18] The human AβPP transgene contained the double Swedish mutations to enhance β-secretase processing and the production of Aβ peptide.[19,20] The Dutch and Iowa mutations were included to yield Aβ peptides with highly vasculotropic properties.[5,6,9] Our initial characterization of these mice showed that they expressed low

Supported by the National Institutes of Health (grant NS36645), the Alzheimer's Association (grant IIRG-02-3995), and ZonMW (Vidi-Vernieuwingsimpuls, 917.46.331).

J.M. and F.X. contributed equally to this work.

Accepted for publication April 18, 2005.

Address reprint requests to Dr. W.E. Van Nostrand, Department of Medicine, HSC T-15/083, Stony Brook University, Stony Brook, NY 11794-8153. E-mail: william.vannostrand@stonybrook.edu.

levels of transgene-encoded human AβPP but developed early-onset and robust accumulation of Aβ in brain, particularly in the cerebral microvasculature.[18] Subsequent analysis showed that Dutch/Iowa mutant Aβ peptides are poorly cleared from brain, across the blood-brain barrier, into the circulation and that this deficiency was primarily due to diminished low-density lipoprotein-1 (LRP-1)-mediated transport across the blood-brain barrier in the cerebral microvasculature.[18,21]

In the present study, we investigated the temporal development of cerebral vascular amyloid and its associated pathology in Tg-SwDI mice. We show that with increasing age there is extensive accumulation of fibrillar vascular amyloid, particularly in cerebral microvessels but with lesser involvement of larger meningeal vessels. Progressive accumulation of cerebral vascular amyloid was associated with reduced microvessel densities, vascular cell apoptosis, and vascular cell loss. Notably, there was a significant presence of neuroinflammatory cells strongly associated with the cerebral microvascular amyloid. Tg-SwDI mice also exhibited elevated levels of the inflammatory cytokines interleukin (IL)-1β and IL-6. These findings support a role for cerebral microvascular amyloid in promoting localized neuroinflammation and suggest that Tg-SwDI are a unique model to investigate these pathological processes associated with microvascular CAA in AD and related disorders.

Materials and Methods

Animals

Generation of Tg-SwDI transgenic mice on a pure C57BL/6 background was recently described.[18] These mice express low levels of human Swedish/Dutch/Iowa mutant AβPP in neurons under control of the mouse Thy1.2 promoter. Heterozygous line B Tg-SwDI and nontransgenic, littermate control C57BL/6 mice ranging from 3 to 24 months of age were used in this study. All work with animals followed National Institutes of Health guidelines and was approved by Stony Brook University Institutional Animal Care and Use Committee.

Histology

Mice were sacrificed at specific ages and the brains were removed and bisected through the mid-sagittal plane. Cerebral hemispheres were immersion-fixed with 70% ethanol overnight and subjected to increasing sequential dehydration in ethanol, followed by xylene treatment and embedding in paraffin. Sagittal sections were cut at 10-μm thickness using a microtome, placed in a flotation water bath at 45°C, and then mounted on Colorfrost/Plus slides (Fisher Scientific, Houston, TX). For quantitative analysis of vessel density and CAA frequency, mouse brain hemispheres were embedded in O.C.T. compound (Sakura Finetek Inc., Torrance, CA) and snap-frozen at −70°C. Sagittal sections were cut at 14-μm thickness using a cryostat, mounted on Colorfrost/Plus slides, fixed in acetone, and stored at −70°C.

Immunohistochemistry

Immunostainings were performed on paraffin sections according to recently published protocols.[18] In brief, sections were deparaffinated and rehydrated. Antigen retrieval was performed by treatment with proteinase K (0.2 mg/ml) for 5 minutes at 22°C for Aβ, collagen type IV, and astrocyte immunostaining, and by 10 mmol/L sodium citrate solution (pH 9.0) for 30 minutes at 90°C in a water-bath for activated microglia immunostaining. Primary antibodies were detected with horseradish peroxidase-conjugated or alkaline phosphatase-conjugated secondary antibodies and visualized either with a stable diaminobenzidine solution (Invitrogen, Carlsbad, CA) or with the fast red substrate system (Spring Bioscience, Fremont, CA), respectively, as substrate. Sections were counterstained with hematoxylin. The following antibodies were used for immunostaining: monoclonal antibody 66.1 (1:300), which recognizes residues 1 to 5 of human Aβ;[22] rabbit polyclonal antibodies specific for Aβ40 or Aβ42 (1:200; Chemicon, Temecula, CA); rabbit polyclonal antibody to collagen type IV (1:100; Research Diagnostics Inc., Flanders, NJ); monoclonal antibody to glial fibrillary acidic protein (GFAP) for identification of astrocytes (1:300, Chemicon); monoclonal antibody 5D4 to keratan sulfate antibody for identification of activated microglia[23,24] (1:200; Seikagaku Corporation, Japan); and biotinylated goat anti-mouse IgG (1:200) and ABC reagent (Vector Laboratories, Burlingame, CA) according to the manufacturer's recommendations.

Confocal Image Analysis

Paraffin sections were deparaffinated, rehydrated, washed in 0.01 mol/L phosphate-buffered saline (PBS), and then antigen retrieval was performed by treatment with proteinase K (0.2 mg/ml) for 10 minutes at 22°C for Aβ and smooth muscle cell α-actin immunolabeling. Nonspecific binding was prevented by incubating with Superblocking buffer in PBS (Pierce, Rockford, IL) containing 0.3% Triton X-100 for 1 hour at 22°C. Primary antibodies were incubated with the brain sections overnight at 4°C. Sections were washed in 0.01 mol/L PBS for three times (5 minutes each), then co-incubated with goat anti-rabbit IgG (Alex 594, 1:2500; Molecular Probes Inc., Eugene, OR) or/and donkey anti-mouse IgG (Alex 488, 1:2500; Molecular Probes, Inc.) for 2 hours in the dark at 22°C. After the first immunofluorescence labeling with primary antibody, detection of fibrillar amyloid was performed by incubating the sections with 1% thioflavin-S in 0.01 mol/L PBS in the dark for 5 minutes at 22°C, followed by washing in 50% ethanol for three times (3 minutes each). Sections were washed, Vectashield (Vector Laboratories) was applied, and a coverslip was placed and sealed with nail polish. The labeled brain sections were examined using an Eclipse E600 confocal laser-scanning microscope (LSM, Nikon, Japan). The primary antibodies used for immunofluorescence labeling were as follows: rabbit polyclonal antibody to Aβ1-28 recognizing residues 1 to 28 of human Aβ (1:200),[25] rabbit polyclonal

antibody to collagen type IV (1:100, Research Diagnostics Inc.), mouse monoclonal antibody to smooth muscle cell α-actin (1:500; Sigma, St. Louis, MO).

Cerebral Vascular Apoptotic Cell Detection

Mice were anesthetized with an intraperitoneal injection of 2.5% avertin and transcardially perfused with cold PBS (0.01 mol/L). Brains were immediately removed and fixed in 10% neutral formalin for 24 hours, followed by xylene treatment and embedding in paraffin. Sections were cut in the sagittal plane at 10-μm thickness using a microtome, deparaffinated, and rehydrated. Terminal dUTP nick-end labeling (TUNEL) was performed on paraffin sections using the ApopTag fluorescein in situ apoptosis detection kit (Chemicon Int. Inc.). In brief, brain sections were rinsed in PBS for 10 minutes, pretreated with proteinase K (20 μg/ml) for 15 minutes at 22°C, and then incubated with equilibration buffer for 10 seconds at 22°C followed by incubating with working strength TdT enzyme at 37°C for 1 hour. Working strength stop/wash buffer was applied for 10 minutes at 22°C. Sections were incubated with working strength anti-digoxigenin-conjugated fluorescein isothiocyanate in the dark for 30 minutes at 22°C. TUNEL-treated sections were incubated with either rabbit polyclonal antibody to Aβ1-28 (1:200) or rabbit polyclonal antibody to collagen type IV (1:100, Research Diagnostics Inc.) for 2 hours, followed by incubating with goat anti-rabbit IgG (Alex 594, 1:2500; Molecular Probes, Inc.) in the dark for 1 hour at 22°C. Brain sections were washed, Vectashield (Vector Laboratories) was applied, and a coverslip was placed and sealed with nail polish. The labeled brain sections were examined using a Eclipse E600 confocal laser-scanning microscope (LSM).

Quantitative Analysis of CAA Frequency and Vessel Density

Groups ($n = 4$) of 3-, 6-, 12-, and 24-month-old Tg-SwDI mice and age-matched nontransgenic littermate C57BL/6 mice were used. Vessel densities and CAA frequency were quantified on systematically sampled serial sections immunostained for collagen type IV or Aβ and collagen type IV double-immunostained sections throughout the regions of interest (every 25th section through the cortex or hippocampus; every 10th section through the thalamus; yielding 8 to 10 sections per region). The Stereologer software system (Systems Planning and Analysis, Alexandria, VA) was used to direct an automated optical fractionator for unbiased vessel counting using a motorized *x*-, *y*-, and *z*-axes microscope stage. A $\times$4 objective was used to define the reference space. The automated random systematic sampling within the reference space was performed using a $\times$40 objective. Unbiased estimation of vessel count per mm^3 was determined in the fronto-temporal cortex, hippocampus, and thalamus. CAA frequency was calculated by counting the percentage of Aβ-associated vessels in the fronto-temporal cortex, thalamic, and subiculum regions.

Electron Microscopic Analysis

Samples were fixed with 2.5% glutaraldehyde in cacodylate buffer for 3 days and postfixed with 1% OsO_4 for 30 minutes. After dehydration with ethanol and subsequent treatment with propylene oxide, the samples were incubated with mixtures of propylene oxide and increasing concentrations of epon until 100% epon resin and embedded in Epon 812 (Electron Microscopy Sciences, Hatfield, PA). Ultrathin sections were cut on a Leica Ultracut and stained with uranyl acetate and lead citrate. Photographs were taken on a Jeol 1200 EX/II electron microscope at 60 kV.

Quantitative Analysis of Astrocytes and Activated Microglia

Total numbers of astrocytes and activated microglia in the fronto-temporal cortex, thalamus, and subiculum regions were estimated using the Stereologer software system (Systems Planning and Analysis). Every 10th section was selected and generated 10 to 15 sections per reference space in a systematic-random manner. Immunopositive cells were counted using the optical fractionator method with the dissector principle and unbiased counting rules.[26] Criteria for counting cells required that cells exhibited positive immunostaining (GFAP for astrocytes and mAb 5D4 to keratan sulfate for activated microglia[23,24]) and morphological features consistent with each cell type. Cells were counted on either the right or the left hemispheres selected at random, and the numbers in each hemisphere doubled to estimate the total cell number for each brain.

Enzyme-Linked Immunosorbent Assay (ELISA) Measurements

Cerebral microvessels and microvascular-depleted brain fractions were isolated from 12-month-old Tg-SwDI mouse forebrains as described.[27] The levels of total Aβ40 and Aβ42 in guanidine extracts prepared from the isolated microvessels and microvascular-depleted parenchymal fractions were determined by sandwich ELISA analysis as described.[28]

For measurement of IL-1β and IL-6 levels, forebrains were isolated from 12-month-old wild-type and Tg-SwDI mice and homogenized in 10 vol of 50 mmol/L Tris-HCl, 150 mmol/L NaCl, pH 7.5, containing protease inhibitor cocktail (SM Biotech, Huntington Station, NY) at 4°C. The samples were centrifuged at 14,000 $\times$ *g* for 50 minutes at 4°C. The supernatants were collected and the protein concentrations were determined using the BCA kit (Pierce). The levels of IL-1β and IL-6 in the samples were determined using mouse IL-1β and IL-6 ELISA kits as described by the manufacturer (Biosource International Inc., Camarillo, CA).

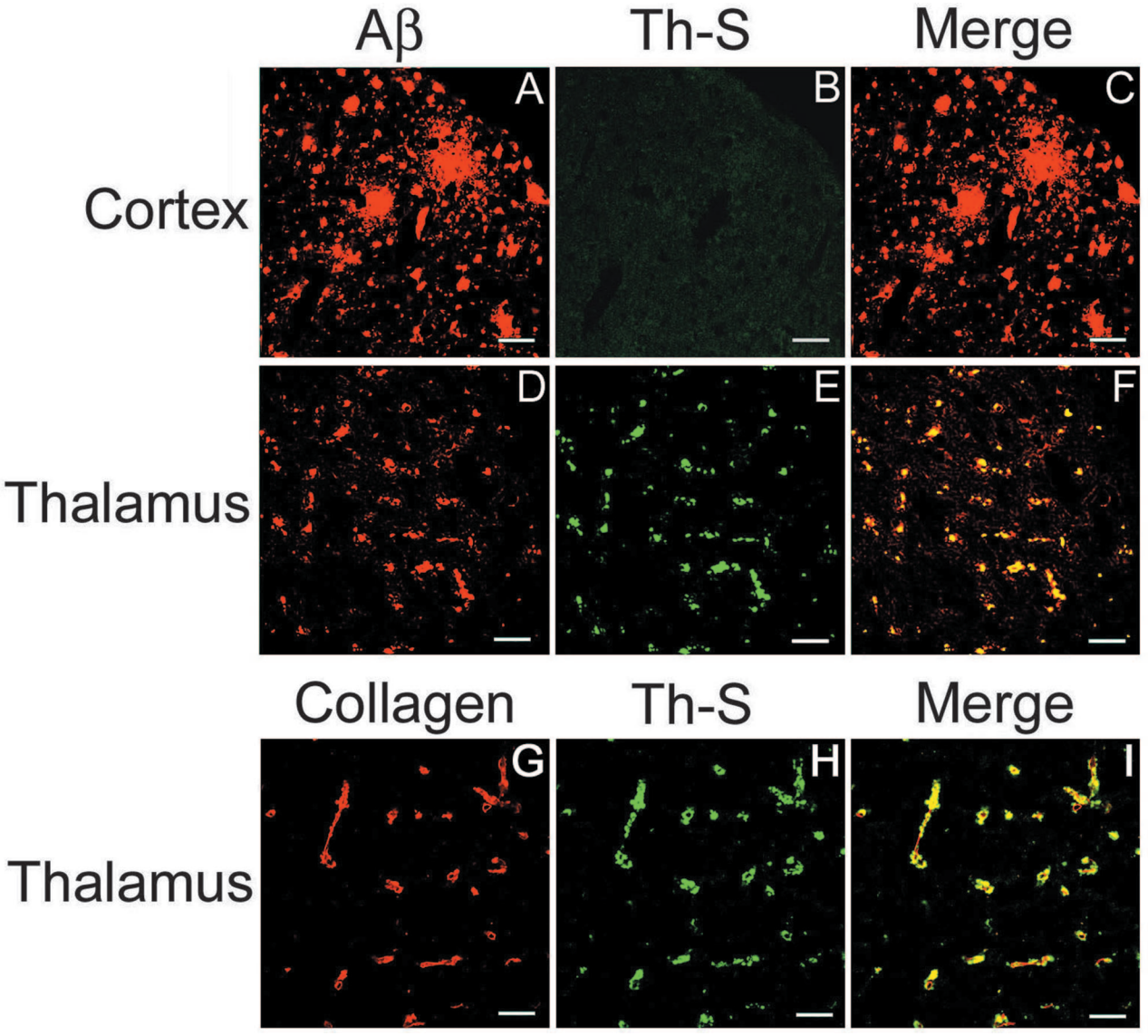

Figure 1. Fibrillar Aβ deposits develop exclusively in the cerebral microvasculature of Tg-SwDI mice. Immunolabeling for Aβ (**A**) and negative thioflavin S staining (**B** and **C**) in the neocortex of 12-month-old Tg-SwDI mice indicates that the abundant diffuse parenchymal deposits in this region are not fibrillar. Immunolabeling for Aβ (**D**) and thioflavin S staining (**E**) in the thalamus co-localize (**F**) identifying abundant microvascular fibrillar amyloid deposits in this region of Tg-SwDI mice. Immunolabeling for collagen IV (**G**) and thioflavin S staining (**H**) in the thalamus co-localize (**I**) confirming the microvascular localization of the fibrillar amyloid in the thalamus of Tg-SwDI mice. Scale bars, 50 μm.

Statistical Analysis

Data were analyzed by Student's *t*-test at $P < 0.05$ significance level.

Results

Regional Extensive Accumulation of Fibrillar Microvascular Amyloid in Tg-SwDI Mice

Tg-SwDI mice express vasculotropic mutant human AβPP in brain and were shown to develop early-onset and robust accumulation of cerebral Aβ.[18] In the fronto-temporal cortex the Aβ accumulates primarily as diffuse parenchymal deposits that do not stain with the fibrillar amyloid dye thioflavin-S (Figure 1; A to C). In contrast, certain regions, such as the thalamus, accumulate large amounts of fibrillar microvascular amyloid (Figure 1; D to F). The co-localization of fibrillar amyloid with the cerebral microvasculature in Tg-SwDI mice was confirmed by double-fluorescent labeling for collagen type IV and thioflavin-S (Figure 1; G to I). To determine which isoforms of Aβ are present in the diffuse parenchymal and fibrillar microvascular Aβ deposits brain tissue sections from 12-month-old Tg-SwDI mice were immunostained with antibodies specific for Aβ40 or Aβ42. Diffuse parenchymal deposits in the fronto-temporal cortex were strongly labeled with antibodies to Aβ40 but only weakly stained with antibodies to Aβ42 (Figure 2, A and B, respectively). However, the fibrillar microvascular amyloid deposits in the thalamic region exhibited prominent immunostaining for both Aβ40 and Aβ42 (Figure 2, C and D, respectively).

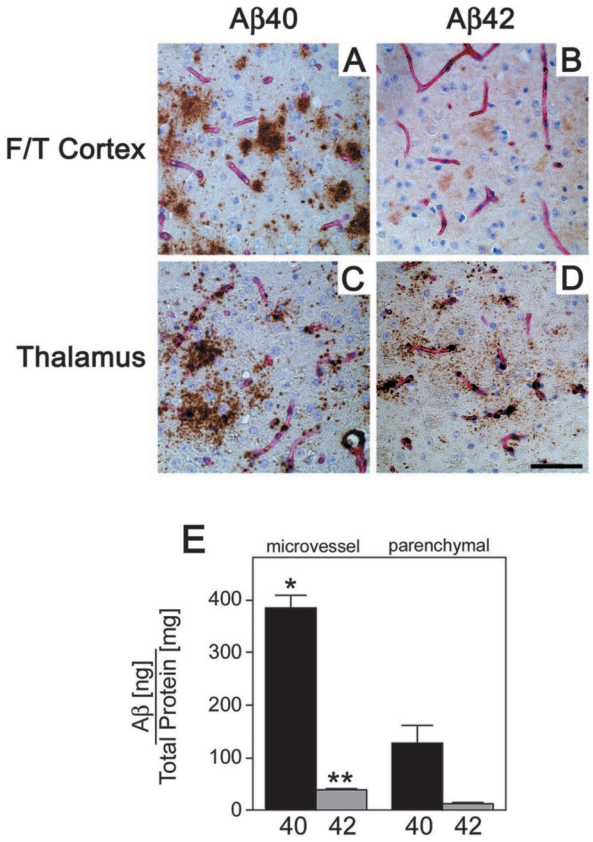

Figure 2. Distribution of Aβ isoforms in parenchymal diffuse and cerebral vascular fibrillar deposits in Tg-SwDI mice. Immunostaining of 12-month-old Tg-SwDI mouse brain sections for collagen IV (red) and Aβ40 or Aβ42 (brown) in the fronto-temporal cortex or thalamus. The diffuse parenchymal deposits showed stronger immunostaining for Aβ40 than Aβ42 (**A** and **B**, respectively) whereas the fibrillar microvascular deposits in the thalamus exhibited strong staining for Aβ40 and Aβ42 (**C** and **D**, respectively). **E:** ELISA analysis for total Aβ40 and Aβ42 in microvessel and nonvascular parenchymal fractions isolated from 12-month-old Tg-SwDI mice. Data shown are the mean ± SD (n = 4 mice). *$P < 0.0002$ and **$P < 0.0001$.

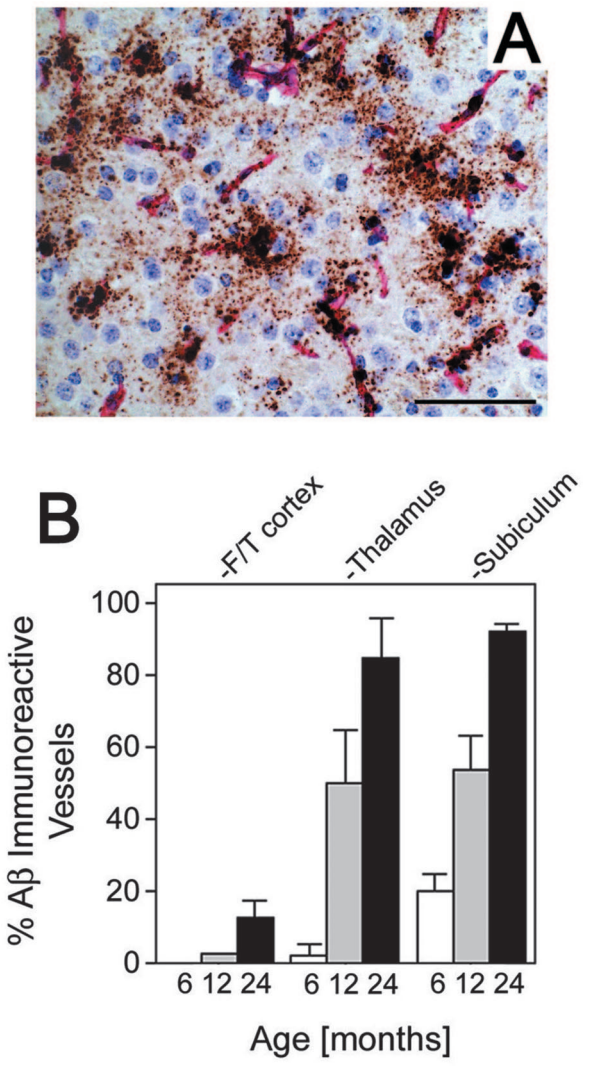

Figure 3. Progressive cerebral microvascular Aβ accumulation in Tg-SwDI mice. **A:** Representative thalamic region from a 12-month-old Tg-SwDI mouse was immunostained for Aβ (brown) and collagen IV (red). **B:** Quantitative stereological measurement of microvascular Aβ deposition in different brain regions of increasing aged Tg-SwDI mice. Data shown are the mean ± SD (n = 4 mice for each age group). Scale bar, 100 μm.

ELISA analysis of extracts from isolated cerebral microvessels and microvascular-depleted parenchymal tissues showed higher levels of Aβ40 than Aβ42 in each fraction (Figure 2E). Although the ratio of Aβ40:Aβ42 was similar in each fraction (≈10:1), the overall amount of each Aβ isoform was significantly higher in the cerebral microvessels.

The regional and temporal development of microvascular CAA was determined using stereological methods to quantitate the numbers of Aβ-immunopositive cerebral microvessels in Tg-SwDI mouse brain sections (Figure 3A). Notable levels of microvascular CAA were observed starting at ~6 months of age in the thalamic and subiculum regions which markedly increased to 85 to 90% affected microvessels at 24 months of age (Figure 3B). The extent of microvascular CAA was substantially lower in the fronto-temporal cortex of Tg-SwDI mice although they exhibited progressive accumulation in this region to a level of ≈15% in 24-month-old animals. Tg-SwDI mice also developed fibrillar amyloid deposits in meningeal vessels showing strong co-localization of Aβ immunoreactivity with thioflavin-S staining (Figure 4; A to C). However, the presence of meningeal vessel amyloid did not appreciably appear until ~12 months of age and was markedly lower than the levels of microvascular amyloid affecting only ≈8% of vessels at 24 months (Figure 4D). Together, these findings show that Tg-SwDI mice exclusively accumulate fibrillar amyloid in the cerebral vasculature with the most extensive presence in the microvasculature of the thalamic and subiculum regions of brain.

Cerebral Vascular Cellular Pathology in Tg-SwDI Mice

We next examined the effect of cerebral microvascular amyloid accumulation on regional cerebral microvessel densities in Tg-SwDI mice. At a young age of 3 months, before accumulation of microvascular amyloid, there was no difference in the microvessel densities between Tg-SwDI and wild-type mice in any of the brain regions

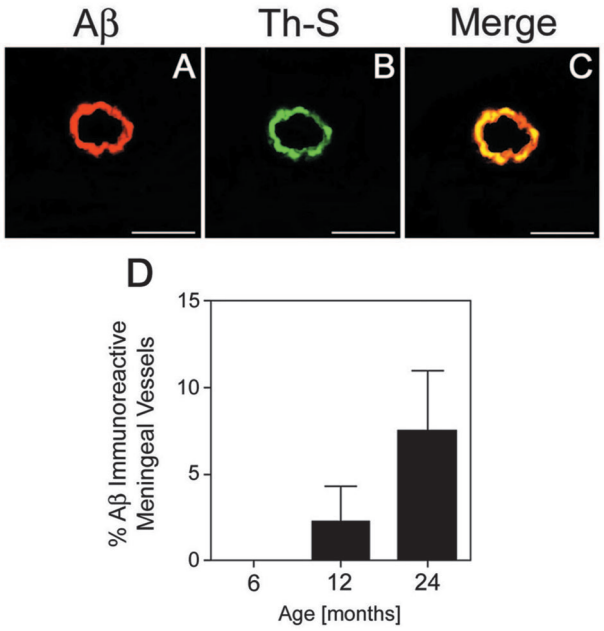

Figure 4. Meningeal vessel Aβ accumulation in Tg-SwDI mice. Immunostaining for Aβ (**A**) and thioflavin S staining (**B**) co-localize (**C**) demonstrating fibrillar amyloid deposition in a meningeal vessel of Tg-SwDI mice. **D:** Quantitative stereological measurement of meningeal vessel Aβ deposition of increasing aged Tg-SwDI mice. Data shown are the mean ± SD ($n = 4$ mice for each age group). Scale bars, 50 μm.

examined (data not shown). Mice were then examined at later ages when regional microvascular amyloid accumulates. In the fronto-temporal cortex, a region with substantial diffuse parenchymal Aβ deposits but only low amounts of cerebral microvascular amyloid (Figures 1 and 3), there was no difference in microvessel densities

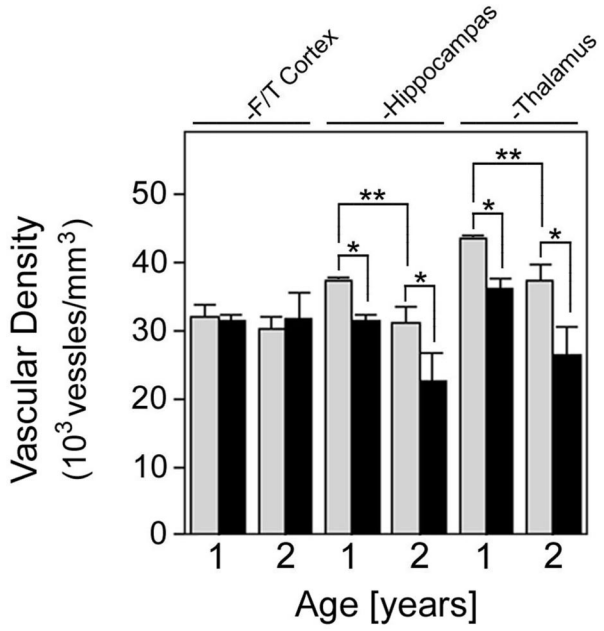

Figure 5. Decreased regional vascular densities in Tg-SwDI mice. Vascular densities were determined in different brain regions of 1- and 2-year-old wild-type mice (**gray bars**) and Tg-SwDI mice (**black bars**) as described in Materials and Methods. Data shown are the mean ± SD ($n = 4$ mice for each group). $^*P < 0.01$ and $^{**}P < 0.02$.

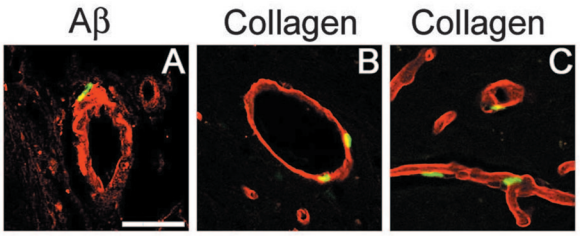

Figure 6. Apoptotic cerebral vascular cells in Tg-SwDI mice. Immunolabeling for Aβ (**A**) or collagen IV (**B** and **C**) in red and TUNEL labeling in green identified apoptotic vascular cells in meningeal vessels (**A** and **B**) and thalamic microvessels (**C**) in 2-year-old Tg-SwDI mice. Scale bar, 50 μm.

between Tg-SwDI and wild-type mice (Figure 5). In contrast, in the hippocampal and thalamic regions, with high microvascular amyloid load, there was a 16% and 17%, respectively, lowering of microvessel densities at 1 year, which increased to 27% and 29%, respectively, at 2 years in Tg-SwDI mice ($P < 0.01$) (Figure 5). In the hippocampus and thalamus a ≈15% decrease ($P < 0.02$) in microvessel densities was observed in wild-type mice as they aged from 1 year to 2 years reflecting a small normal age-related decline in these regions.

Double-labeling experiments, combining immunolabeling for either Aβ or collagen IV and TUNEL staining for apoptotic cells, were performed to identify cerebral vascular cell death in cerebral vessels with amyloid deposition. TUNEL-positive apoptotic cells could be found in the walls of meningeal vessels and co-localized with Aβ or collagen immunostaining in Tg-SwDI mice (Figure 6, A and B, respectively). Similarly, apoptotic cells were identified in thalamic microvessels, a region rich in microvascular amyloid (Figure 6C). Furthermore, the accumulation of amyloid in meningeal vessels was accompanied by a loss of smooth muscle cells in the vessel wall as shown by the depletion of vascular smooth muscle cell α-actin (Figure 7). In contrast, no TUNEL-positive apoptotic cells or smooth muscle cell loss was observed in any cerebral

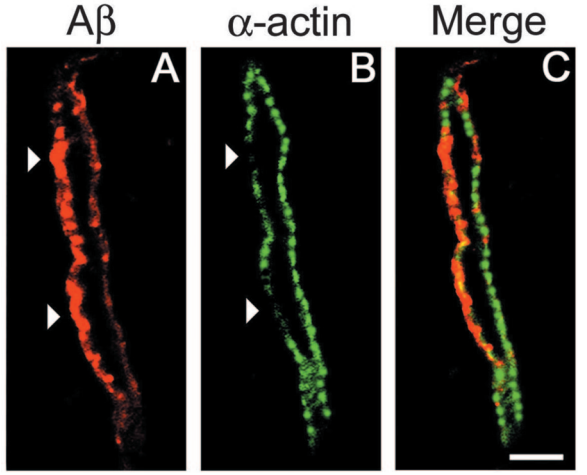

Figure 7. Loss of smooth muscle cells in amyloid-laden meningeal vessels of Tg-SwDI mice. Immunolabeling for Aβ (**A**) and vascular smooth muscle cell α-actin (**B**) in a meningeal vessel of a 2-year-old Tg-SwDI mouse. The **arrowheads** reveal loss of smooth muscle cells in the amyloid-rich regions of the vessel as shown in the merge image (**C**). Scale bar, 50 μm.

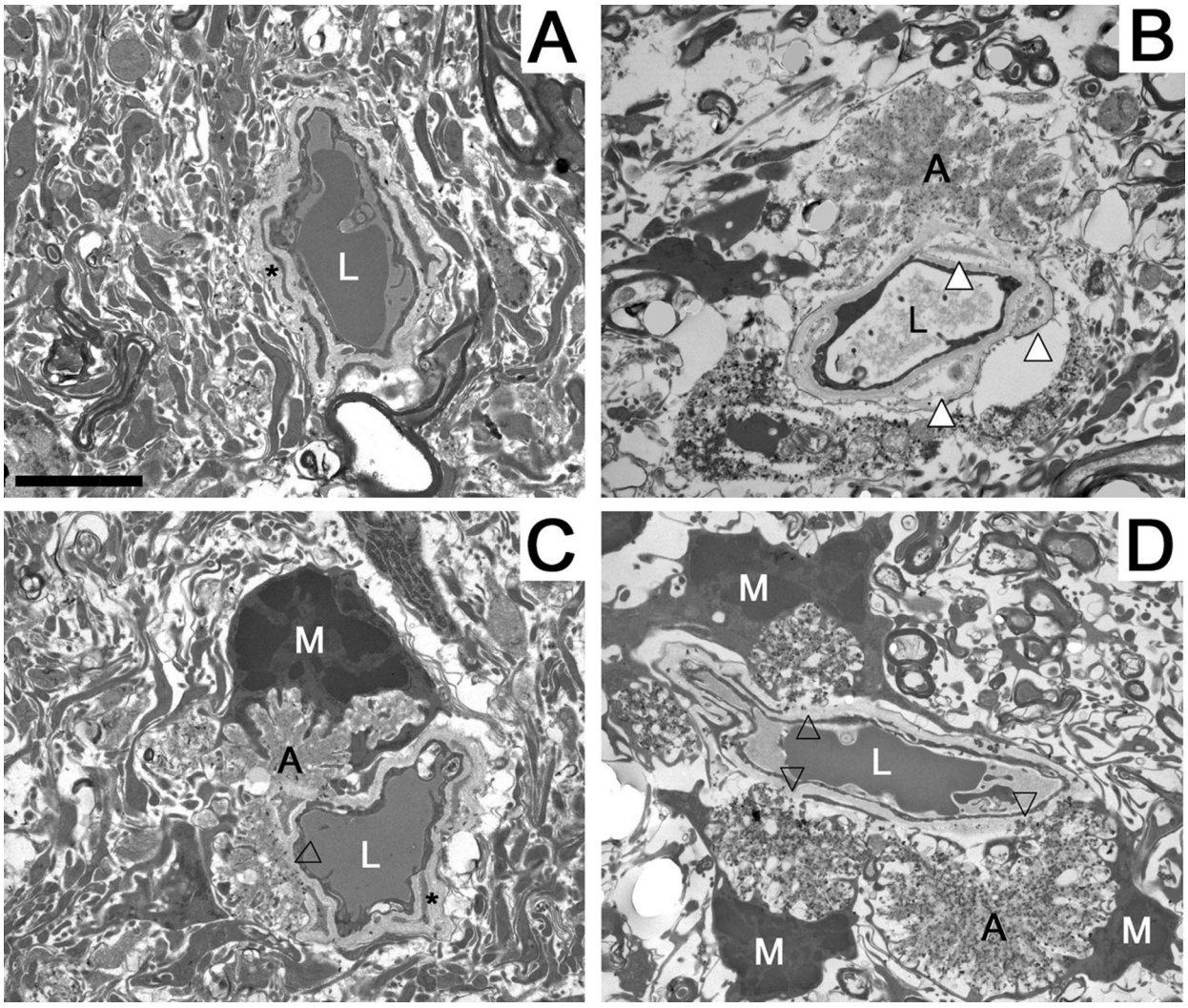

Figure 8. Ultrastructural analysis of cerebral microvascular amyloid deposition in Tg-SwDI mice. **A:** Normal thalamic microvessel in a wild-type mouse. Vessel lumen (L) and vascular basement membrane (*) are identified. **B:** Thalamic microvessel in a Tg-SwDI mouse with an amyloid deposit (A) and degenerating pericytes with swollen vacuoles (**white arrowheads**). **C:** Tg-SwDI cerebral microvessel with amyloid deposition and an engaged microglial cell (M). Initial penetrance of amyloid into the vascular basement membrane is identified by the **open arrowhead**. **D:** Another thalamic microvessel in a Tg-SwDI mouse with more extensive amyloid deposition extending into the surrounding parenchyma, several sites of amyloid breaching the vascular basement membrane, and several engaged microglial cells. Scale bar, 2.5 μm.

vessels of nontransgenic wild-type mice (data not shown).

Electron microscopy analysis was performed for the ultrastructural characterization of cerebral microvascular amyloid deposition in Tg-SwDI mice. Figure 8A shows a normal thalamic microvessel in a 12-month-old wild-type mouse unaffected by amyloid deposition. In contrast, Figure 8B depicts a thalamic microvessel from a similarly aged Tg-SwDI mouse presenting a fibrillar amyloid deposit adhering to the microvessel. Although the endothelial cells appear unperturbed pericyte degeneration is observed with less electron-dense cytoplasm containing large vacuoles. In another example, a microvessel-associated amyloid deposit is seen with initial signs of penetrating the vascular basement membrane (Figure 8C). In this same image a microglial cell can be seen engulfing the amyloid deposit. Another thalamic microvessel in the same Tg-SwDI mouse showed more advanced pathology with multiple fibrillar amyloid deposits extending into the adventitia, reduced vessel lumen, several areas of amyloid penetrating the basement membrane, and multiple microglia interacting with the amyloid deposits (Figure 8D).

Progressive Accumulation of Cerebral Microvascular Amyloid-Associated Neuroinflammatory Cells in Tg-SwDI Mice

The ultrastructural analysis indicated that neuroinflammatory cells may be associated with cerebral microvascular amyloid deposition in Tg-SwDI mice. Therefore, we performed double-immunolabeling experiments to identify cerebral microvessels and astrocytes in different brain regions of 12-month-old wild-type and Tg-SwDI mice. Modest astrocyte staining was observed in all examined brain regions of the wild-type mice (Figure 9; A to C). However, Tg-SwDI mice exhibited pronounced numbers of strongly GFAP-positive reactive astrocytes that were

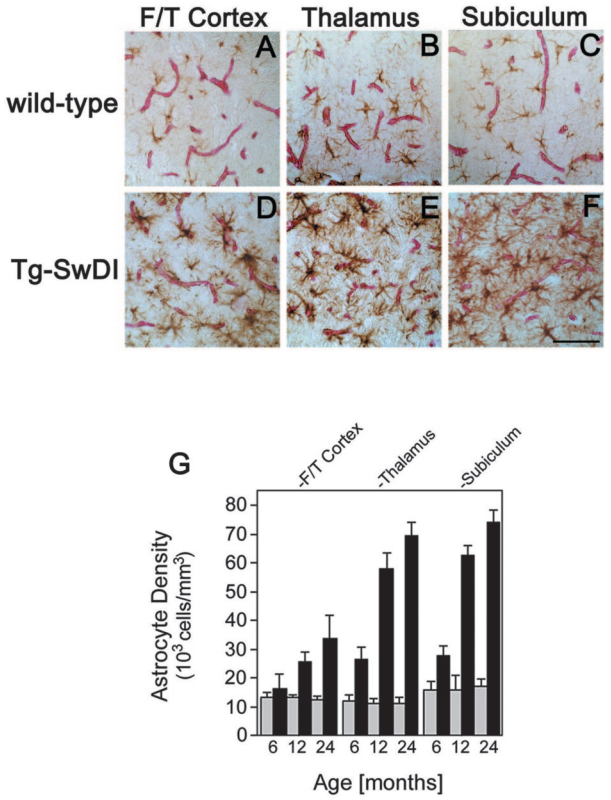

Figure 9. Increased cerebral microvascular-associated reactive astrocytes in Tg-SwDI mice. Immunostaining for GFAP (brown) and collagen IV (red) for identifying astrocytes and microvessels, respectively, in different brain regions of 1-year-old wild-type mice (**A–C**) and Tg-SwDI mice (**D–F**). **G:** Quantitative stereological measurement of astrocyte densities in brain regions of increasing aged wild-type mice (**gray bars**) and Tg-SwDI mice (**black bars**). Data shown are mean ± SD ($n = 4$ mice for each group). Scale bar, 50 μm.

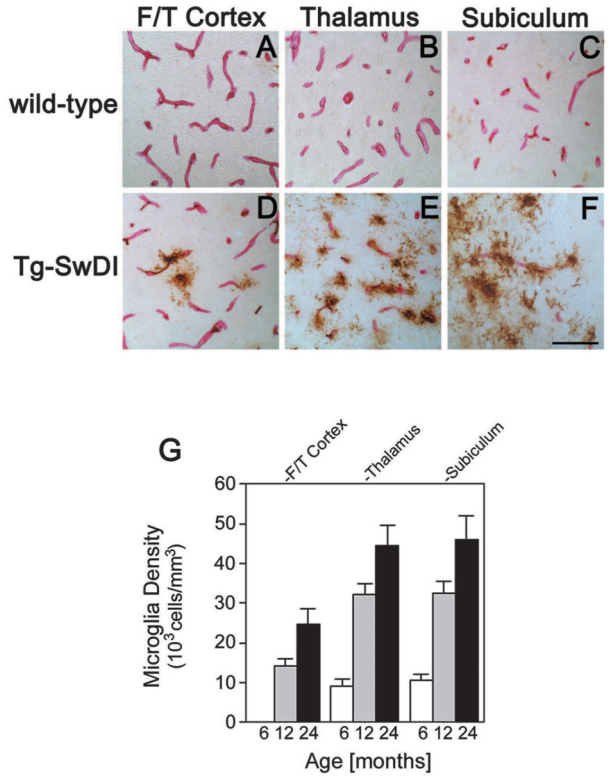

Figure 10. Increased cerebral microvascular-associated activated microglia in Tg-SwDI mice. Immunostaining for mAb 5D4 (brown) and collagen IV (red) for identifying activated microglia and microvessels, respectively, in different brain regions of 1-year-old wild-type mice (**A–C**) and Tg-SwDI mice (**D–F**). **G:** Quantitative stereological measurement of activated microglial densities in brain regions of increasing aged Tg-SwDI mice. Data shown are mean ± SD ($n = 4$ mice for each group). Scale bar, 50 μm.

particularly associated with amyloid-laden microvessels (Figure 9; D to F). Quantitative, unbiased stereological analysis was performed to determine the numbers of astrocytes in the different brain regions of 6- to 24-month-old wild-type and Tg-SwDI mice (Figure 9G). Wild-type mice exhibited similar numbers of astrocytes in all of the examined brain regions and these numbers did not change with increasing age. In contrast, Tg-SwDI showed a pronounced elevation in the numbers of astrocytes that dramatically increased with age. Moreover, larger numbers of reactive astrocytes were found in the brain regions with the highest amounts of cerebral microvascular fibrillar amyloid (ie, thalamus and subiculum).

Similarly, we next performed double-immunolabeling experiments to identify cerebral microvessels and activated microglia in different brain regions of 12-month-old wild-type and Tg-SwDI mice. Wild-type mice showed no activated microglia in any of the brain regions (Figure 10; A to C). On the other hand, Tg-SwDI mice presented numerous activated microglia in the different brain regions, again strongly associated with the amyloid-laden microvessels (Figure 10; D to F). This finding is consistent with the ultrastructural co-localization of activated microglia with the cerebral microvascular fibrillar amyloid deposits (Figure 8, C and D). We next performed quantitative, unbiased stereological analysis to determine the numbers of activated microglia in the different brain regions of 6- to 24-month-old wild-type and Tg-SwDI mice (Figure 10G). No activated microglia were found in any brain region of wild-type mice of any age (data not shown). In contrast, Tg-SwDI showed robust numbers of activated microglia that markedly increased with age. Again, larger numbers of activated microglia were found in the brain regions with the highest amounts of cerebral microvascular fibrillar amyloid (ie, thalamus and subiculum).

Because increased numbers of neuroinflammatory cells were found in the presence of microvascular amyloid in Tg-SwDI mice we next measured the levels of IL-1β and IL-6, two cerebral microvascular-associated inflammatory cytokines (Figure 11).[29,30] Twelve-month-old Tg-SwDI mice exhibited ~5- and 10-fold increased levels of IL-1β and IL-6, respectively, compared with same aged wild-type mice. Together, these findings indicate that neuroinflammatory reactive astrocytes and activated microglia are strongly associated with cerebral microvascular fibrillar amyloid and certain neuroinflammatory cytokines are elevated in Tg-SwDI mice.

Discussion

The present findings show that Tg-SwDI mice develop early-onset fibrillar Aβ deposits exclusively in the cere-

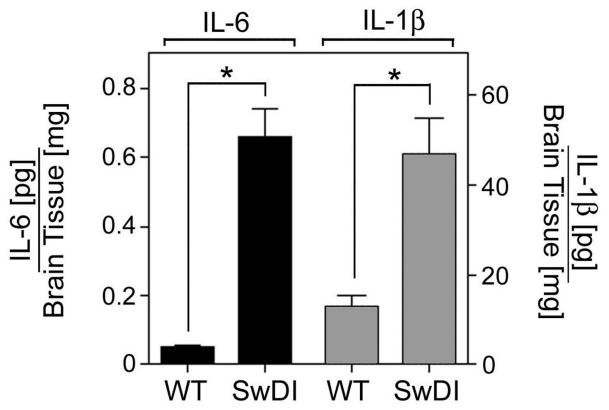

Figure 11. Elevated levels of inflammatory cytokines in Tg-SwDI mouse brain. The levels of IL-1β (**gray bars**) and IL-6 (**black bars**) in soluble brain extracts prepared from 12-month-old wild-type and Tg-SwDI mice were determined by ELISA analysis as described in Materials and Methods. Data shown are mean ± SD ($n = 5$ mice for each group). *$P < 0.0001$.

bral vasculature with only diffuse Aβ deposition in the brain parenchyma. In certain brain regions, such as the thalamus and subiculum, microvascular Aβ deposition becomes very extensive affecting ≈90% of the microvessels by 2 years of age. Although fibrillar amyloid is also found in some larger meningeal vessels, the frequency of these affected vessels is much lower. The vascular amyloid is composed of both Aβ40 and Aβ42 human Dutch/Iowa mutant peptides. In brain regions with extensive vascular amyloid accumulation there are significant decreases in vascular densities, microvascular pericyte degeneration, presence of apoptotic vascular cells, and loss of vessel wall smooth muscle cells indicating the degenerative effects of vascular amyloid in Tg-SwDI mice. The deposition of cerebral microvascular amyloid was accompanied by large increases in the numbers of neuroinflammatory reactive astrocytes and activated microglia as well as elevated cerebral levels of the neuroinflammatory cytokines IL-1β and IL-6. Together, these results suggest that the Tg-SwDI model is a unique and invaluable paradigm for investigating cerebral vascular Aβ deposition and its effects on vessel wall degeneration and vascular amyloid-induced neuroinflammation.

Previously, several different human AβPP transgenic mice have been generated that produce wild-type Aβ peptides in brain.[31–35] Most of these transgenic mouse lines have been shown to develop diffuse and fibrillar parenchymal plaque deposits with varying degrees of subsequent vascular amyloid formation. Recently, Herzig and colleagues[36] reported the generation of transgenic mice that express Dutch mutant human AβPP and produce E22Q Dutch mutant Aβ peptides in brain. In this model, Dutch mutant Aβ was found to accumulate only in the cerebral vasculature of aged (>24 months) mice indicating the vasculotropic nature of the Dutch mutation. In our recently generated Tg-SwDI mice, the presence of the dual Dutch and Iowa vasculotropic mutations (E22Q,D23N) within Aβ substantially accelerates the accumulation of microvascular amyloid with appreciable amounts observed at ~6 months.[18] Throughout time, larger meningeal vessels of older Tg-SwDI mice also accumulate amyloid, but to a much lesser extent than in cerebral microvessels. In addition to abundant fibrillar vascular amyloid, numerous diffuse parenchymal Aβ deposits develop in Tg-SwDI mice consistent with the Aβ pathology found in patients with either the Dutch or Iowa familial CAA disorders.[9,37,38] The early-onset and robust accumulation of cerebral microvascular amyloid in Tg-SwDI mice developed despite the low, subendogenous expression of transgene-encoded human SwDI mutant AβPP and low production of Dutch/Iowa mutant Aβ peptides in brain.[18] Because microvascular deposited Aβ peptides are derived from a neuronal source in Tg-SwDI mice this supports the concept of Aβ drainage from parenchymal interstitial fluid to the capillary walls.[39,40] This process, in conjunction with the ineffective clearance of Dutch/Iowa mutant Aβ from brain across the capillary blood-brain barrier into the circulation,[18,21] likely leads to the extensive formation of cerebral microvascular Aβ deposition that penetrates the immediate surrounding parenchyma, also known as "dyshoric angiopathy," in Tg-SwDI mice.

Subtle, but significant, decreased cerebral microvessel densities were observed in aged wild-type mice. Although the precise mechanism responsible for this small decline is unclear it appears to reflect normal cerebral vascular declines previously reported in the aged rodent and human brain.[41–47] However, more robust decreases in cerebral microvessel densities were noted in brain regions of Tg-SwDI mice with high amounts of microvascular amyloid. Similar findings have been reported in another human AβPP transgenic mouse model as well as in AD.[42,47] In the presence of vascular amyloid these decreases likely result from the cerebral vascular degenerative effects, and possible anti-angiogenic properties, of deposited Aβ peptides.[47] Indeed, the accumulation of cerebral vascular amyloid in Tg-SwDI mice led to the decreased integrity of the basement membrane, degeneration of microvascular pericytes, presence of apoptotic cerebral vascular cells, and loss of smooth muscle cells in some larger meningeal vessels. These pathological consequences of cerebral vascular amyloid observed in Tg-SwDI mice are in strong agreement with the pathology found in amyloidotic cerebral vessels of patients afflicted with the familial Dutch-type or Iowa-type CAA disorders.[9,37,38,48–50] Moreover, the present findings are highly consistent with numerous previous reports describing the pathogenic effects of deposited fibrillar Aβ in human cerebral vascular cell cultures. For example, deposited fibrillar Aβ, but not soluble Aβ, promotes cell degeneration and apoptosis in primary cultures of cerebrovascular smooth muscle cells and brain microvascular pericytes.[51–53] Similarly, deposited fibrillar Aβ was shown to stimulate the degradation of vascular smooth muscle cell α-actin in cultured human cerebrovascular smooth muscle cells.[53]

Our findings provide significant evidence demonstrating that cerebral microvascular fibrillar amyloid deposition can exclusively induce local neuroinflammation in Tg-SwDI mice in the absence of parenchymal plaque fibrillar amyloid deposition. For example, the levels of IL-1β and IL-6, two inflammatory cytokines reported to be

increased in AD amyloid-containing cerebral microvessels,[29,30] were strongly elevated in Tg-SwDI mouse brain. More specifically, reactive astrocytes and activated microglia were found to be tightly associated with the cerebral microvascular amyloid deposition. As shown in Tg-SwDI mice, the numbers of these neuroinflammatory cells were highest in the regions with the most extensive microvascular amyloid (ie, thalamus and subiculum) and increased in conjunction with the increase in cerebral microvascular Aβ load in all brain regions. The intimate association of reactive astrocytes and activated microglia with cerebral microvascular amyloid in Tg-SwDI mice is highly consistent with the cerebral vascular localization of these neuroinflammatory cells in patients with the Dutch- or Iowa-type familial CAA disorders.[12,14–17] In these disorders, as in the Tg-SwDI mice, the induction of a neuroinflammatory reaction appears to correlate with amyloid extending from the vessel wall into the surrounding parenchymal tissues.

Recent studies have suggested that treatments designed to reduce cerebral vascular amyloid-induced neuroinflammation in afflicted individuals have improved the dementia associated with this particular pathology.[54–56] Because cerebral vascular amyloid pathology is also commonly observed in AD, this target may have further implications in combined treatment strategies for this neurodegenerative condition and its related disorders. The present results indicate that Tg-SwDI mice provide a unique model to further investigate the role of cerebral microvascular amyloidosis and its accompanying neuroinflammatory response.

References

1. Selkoe DJ: Alzheimer's disease: genes, proteins, and therapy. Physiol Rev 2001, 81:741–766
2. Jellinger KA: Alzheimer's disease and cerebrovascular pathology: an update. J Neural Transm 2002, 109:813–836
3. Vinters HV, Farag ES: Amyloidosis of cerebral arteries. Adv Neurol 2003, 92:105–112
4. Selkoe DJ: Deciphering the genesis and fate of amyloid beta-protein yields novel therapies for Alzheimer disease. J Clin Invest 2002, 110:1375–1381
5. Levy E, Carman MD, Fernandez-Madrid IJ, Power MD, Lieberburg I, van Duinen SG, Bots GTAM, Luyendijk W, Frangione B: Mutation of the Alzheimer's disease amyloid gene in hereditary cerebral hemorrhage, Dutch type. Science 1990, 248:1124–1126
6. Van Broeckhoven C, Haan J, Bakker E, Hardy JA, Van Hul W, Wehnert A, Vegter Van der Vlis M, Roos RA: Amyloid beta protein precursor gene and hereditary cerebral hemorrhage with amyloidosis (Dutch). Science 1990, 248:1120–1122
7. Hendriks L, van Duijn CM, Cras P, Cruts M, Van Hul W, van Harskamp F, Warren A, McInnis MG, Antonarakis SE, Martin JJ, Hofman A, Van Broeckhoven C: Presenile dementia and cerebral haemorrhage linked to a mutation at codon 692 of the beta-amyloid precursor protein gene. Nat Genet 1992, 1:218–221
8. Tagliavini F, Rossi G, Padovani A, Magoni M, Andora G, Sgarzi M, Bizzi A, Savioardo M, Carella F, Morbin M, Giaccone G, Bugiani O: A new BetaPP mutation related to hereditary cerebral haemorrhage. Alzheimer's Rep 1999, 2:S28
9. Grabowski TJ, Cho HS, Vonsattel JPG, Rebeck GW, Greenberg SM: Novel amyloid precursor protein mutation in an Iowa family with dementia and severe cerebral amyloid angiopathy. Ann Neurol 2001, 49:697–705
10. Neuropathology Group of the Medical Research Council Cognitive Function and Ageing Study (MRC CFAS): Pathological correlates of late-onset dementia in a multicentre, community-based population in England and Wales. Lancet 2001, 357:169–175
11. Thal DR, Ghebremedhin E, Orantes M, Wiestler OD: Vascular pathology in Alzheimer's disease: correlation of cerebral amyloid angiopathy and arteriosclerosis/lipohyalinosis with cognitive decline. J Neuropathol Exp Neurol 2003, 62:1287–1301
12. Maat-Schieman ML, van Duinen SG, Rozemuller AJ, Haan J, Roos RA: Association of vascular amyloid beta and cells of the mononuclear phagocyte system in hereditary cerebral hemorrhage with amyloidosis (Dutch) and Alzheimer disease. J Neuropathol Exp Neurol 1997, 56:273–284
13. Bailey TL, Rivara CB, Rocher AB, Hof PR: The nature and effects of cortical microvascular pathology in aging and Alzheimer's disease. Neurol Res 2004, 26:573–578
14. Vinters HV, Natte R, Maat-Schieman ML, van Duinen SG, Hegeman-Kleinn I, Welling-Graafland C, Haan J, Roos RA: Secondary microvascular degeneration in amyloid angiopathy of patients with hereditary cerebral hemorrhage with amyloidosis, Dutch type (HCHWA-D). Acta Neuropathol 1998, 95:235–244
15. Vinters HV: Cerebral amyloid angiopathy: a microvascular link between parenchymal and vascular dementia? Ann Neurol 2001, 49:691–692
16. Shin Y, Cho HS, Rebeck GW, Greenberg SM: Vascular changes in Iowa-type hereditary cerebral amyloid angiopathy. Ann NY Acad Sci 2002, 977:245–251
17. Maat-Schieman MLC, Yamaguchi H, Hegeman-Kleinn I, Welling-Graafland C, Natte R, Roos RAC, van Duinen SG: Glial reactions and the clearance of amyloid β protein in the brains of patients with hereditary cerebral hemorrhage with amyloidosis-Dutch type. Acta Neuropathol 2004, 107:389–398
18. Davis J, Xu F, Deane R, Romanov G, Previti ML, Zeigler K, Zlokovic BV, Van Nostrand WE: Early-onset and robust cerebral microvascular accumulation of amyloid beta-protein in transgenic mice expressing low levels of a vasculotropic Dutch/Iowa mutant form of amyloid β-protein precursor. J Biol Chem 2004, 279:20296–20306
19. Mullan M, Crawford F, Axelman K, Houlden H, Lilius L, Winblad B, Lannefelt L: A pathogenic mutation for probable Alzheimer's disease in the APP gene at the N-terminus of beta-amyloid. Nat Genet 1992, 1:345–347
20. Citron M, Oltersdorf T, Haass C, McConlogue L, Hung AY, Seubert P, Vigo-Pelfrey C, Lieberberg I, Selkoe DJ: Mutation of the β-amyloid precursor protein in familial Alzheimer's disease increases β-protein production. Nature 1992, 360:672–674
21. Deane R, Wu Z, Sagare A, Davis J, Yan SD, Hamm K, Xu F, Parisi M, LaRue B, Hu HW, Spijkers P, Guo H, Song X, Lenting PJ, Van Nostrand WE, Zlokovic BV: LRP-amyloid beta-peptide (Abeta) interaction regulates differential brain efflux of Abeta isoforms. Neuron 2004, 43:333–344
22. Deane R, Du Yan S, Submamaryan RK, LaRue B, Jovanovic S, Hogg E, Welch D, Manness L, Lin C, Yu J, Zhu H, Ghiso J, Frangione B, Stern A, Schmidt AM, Armstrong DL, Arnold B, Liliensiek B, Nawroth P, Hofman F, Kindy M, Stern D, Zlokovic B: RAGE mediates amyloid beta-peptide transport across the blood-brain barrier and accumulation in brain. Nat Med 2003, 9:907–913
23. Bertolotto A, Manzardo E, Iudicello M, Guglielmone R, Riccio A: Keratan sulphate is a marker of differentiation of ramified microglia. Brain Res Dev Brain Res 1995, 26:233–241
24. Wilms H, Wollmer MA, Sievers J: In vitro-staining specificity of the antibody 5-D-4 for microglia but not for monocytes and macrophages indicates that microglia are a unique subgroup of the myelomonocytic lineage. J Neuroimmun 1999, 98:89–95
25. Davis-Salinas J, Saporito-Irwin SM, Donovan FM, Cunningham DD, Van Nostrand WE: Thrombin receptor activation induces secretion and nonamyloidogenic processing of amyloid beta-protein precursor. J Biol Chem 1994, 269:22623–22627
26. Long JM, Kalehua AN, Muth NJ, Calhoun ME, Jucker M, Hengemihle JM, Ingram DK, Mouton PR: Stereological estimation of total microglia number in mouse hippocampus. J Neurosci Methods 1998, 84:101–108
27. Zlokovic BV, Mackic JB, Wang L, McComb JG, McDonough A: Differential expression of Na,K-ATPase alpha and beta subunit isoforms at the blood-brain barrier and the choroid plexus. J Biol Chem 1993, 268:8019–8025

28. Johnson-Wood K, Lee M, Motter R, Hu K, Gordon G, Barbour R, Khan K, Gordon M, Tan H, Games D, Lieberburg I, Schenk D, Seubert P, McConlogue L: Amyloid precursor protein processing and Aβ42 deposition in a transgenic mouse model of Alzheimer's disease. Proc Natl Acad Sci USA 1997, 94:1550–1555
29. Grammas P, Ovase R: Inflammatory factors are elevated in brain microvessels in Alzheimer's disease. Neurobiol Aging 2001, 22:837–842
30. Grammas P, Ovase R: Cerebrovascular transforming growth factor-beta contributes to neuroinflammation in the Alzheimer's disease brain. Am J Pathol 2002, 160:1583–1587
31. Games D, Adams D, Alessandrini R, Barbour R, Berthelette P, Blackwell C, Carr T, Clemens J, Donaldson T, Gillespie F, Guido T, Hagopian S, Johnson-Wood K, Khan K, Lee M, Leibowitz P, Lieberberg I, Little S, Masliah E, McConlogue L, Montoya-Zavala M, Mucke L, Paganini L, Penniman E, Power M, Schenk D, Seubert P, Snyder B, Soriano F, Tan H, Vitale J, Wadsworth S, Wolozin B, Zhao J: Alzheimer-type neuropathology in transgenic mice overexpressing V717F beta-amyloid precursor protein. Nature 1995, 373:523–527
32. Hsiao K, Chapman P, Nilsen S, Eckman C, Harigaya Y, Younkin S, Yang F, Cole G: Correlative memory deficits, Aβ elevation, and amyloid plaques in transgenic mice. Science 1996, 274:99–102
33. Calhoun ME, Burgermeister P, Phinney AL, Stalder M, Tolnay M, Wiederhold KH, Abramowski D, Sturchler-Pierrat C, Sommer B, Staufenbiel M, Jucker M: Neuronal overexpression of mutant amyloid precursor protein results in prominent deposition of cerebrovascular amyloid. Proc Natl Acad Sci USA 1999, 96:14088–14093
34. Van Dorpe J, Smeijers L, Dewachter I, Nuyens D, Spittaels K, Van den Haute C, Mercken M, Moechars D, Laenen I, Kuiperi C, Bruynseels K, Tesseur I, Loos R, Vanderstichele H, Checler F, Sciot R, Van Leuven F: Prominent cerebral amyloid angiopathy in transgenic mice overexpressing the London mutant of human APP in neurons. Am J Pathol 2000, 157:1283–1298
35. Chishti MA, Yang DS, Janus C, Phinney AL, Horne P, Pearson J, Strome R, Zuker N, Loukides J, French J, Turner S, Lozza G, Grilli M, Kunicki S, Morissette C, Paquette J, Gervais F, Bergeron C, Fraser PE, Carlson GA, George-Hyslop PS, Westaway D: Early-onset amyloid deposition and cognitive deficits in transgenic mice expressing a double mutant form of amyloid precursor protein 695. J Biol Chem 2001, 276:21562–21570
36. Herzig MC, Winkler DT, Burgermeister P, Pfeifer M, Kohler E, Schmidt SD, Danner S, Abramowski D, Sturchler-Pierrat C, Burki K, van Duinen SG, Maat-Schieman ML, Staufenbiel M, Mathews PM, Jucker M: Abeta is targeted to the vasculature in a mouse model of hereditary cerebral hemorrhage with amyloidosis. Nat Neurosci 2004, 7:954–960
37. Rozemuller AJM, Roos RAC, Bots GTAM, Kamphorst W, Eikelenboom P, Van Nostrand WE: Distribution of beta/A4 and amyloid precursor protein in hereditary cerebral hemorrhage with amyloidosis-Dutch type and Alzheimer's disease. Am J Pathol 1993, 142:1449–1457
38. Wattendorff AR, Frangione B, Luyendijk W, Bots GTAM: Hereditary cerebral haemorrhage with amyloidosis, Dutch type (HCHWA-D): clinicopathological studies. J Neurol Neurosurg Psychiatry 1995, 59:699–705
39. Weller RO, Massey A, Newman TA, Hutchings M, Kuo YM, Roher AE: Cerebral amyloid angiopathy: amyloid beta accumulates in putative interstitial fluid drainage pathways in Alzheimer's disease. Am J Pathol 1998, 153:725–733
40. Weller RO, Massey A, Kuo YM, Roher AE: Cerebral amyloid angiopathy: accumulation of A beta in interstitial fluid drainage pathways in Alzheimer's disease. Ann NY Acad Sci 2000, 903:110–117
41. Wilkinson JH, Hopewell JW, Reinhold HS: A quantitative study of age-related changes in the vascular architecture of the rat cerebral cortex. Neuropathol Appl Neurobiol 1981, 7:451–462
42. Mann DM, Eaves NR, Marcyniuk B, Yates PO: Quantitative changes in cerebral cortical microvasculature in ageing and dementia. Neurobiol Aging 1986, 7:321–330
43. Bell MA, Ball MJ: Neuritic plaques and vessels of visual cortex in aging and Alzheimer's dementia. Neurobiol Aging 1990, 11:359–370
44. Abernethy WB, Bell MA, Morris M, Moody DM: Microvascular density of the human paraventricular nucleus decreases with aging but not hypertension. Exp Neurol 1993, 121:270–274
45. Sonntag WE, Lynch CD, Cooney PT, Hutchins PM: Decreases in cerebral microvasculature with age are associated with the decline in growth hormone and insulin-like growth factor 1. Endocrinology 1997, 138:3515–3520
46. Lynch CD, Cooney PT, Bennett SA, Thornton PL, Khan AS, Ingram RL, Sonntag WE: Effects of moderate caloric restriction on cortical microvascular density and local cerebral blood flow in aged rats. Neurobiol Aging 1999, 20:191–200
47. Paris D, Patel N, DelleDonne A, Quadros A, Smeed R, Mullan M: Impaired angiogenesis in a transgenic mouse model of cerebral amyloidosis. Neurosci Lett 2004, 366:80–85
48. Coria F, Larrondo-Lillo M, Frangione B: Degeneration of smooth muscle cells in beta-amyloid angiopathies. J Neuropathol Exp Neurol 1989, 48:368–375
49. Kawai M, Kalaria RN, Cras P, Siedlak SL, Velasco ME, Shelton ER, Chan HW, Greenberg BD, Perry G: Degeneration of vascular muscle cells in cerebral amyloid angiopathy of Alzheimer disease. Brain Res 1993, 623:142–146
50. Vinters HV, Secor DL, Read SL, Frazee JG, Tomiyasy U, Stanley TM, Ferreiro JA, Akers MA: Microvasculature in brain biopsy specimens from patients with Alzheimer's disease: an immunohistochemical and ultrastructural study. Ultrastruct Pathol 1994, 18:333–348
51. Van Nostrand WE, Melchor J, Ruffini L: Pathologic cell surface amyloid beta-protein fibril assembly in cultured human cerebrovascular smooth muscle cells. J Neurochem 1997, 69:216–223
52. Verbeek MM, de Waal RMW, Schipper JJ, Van Nostrand WE: Rapid degeneration of cultured human brain pericytes by amyloid beta protein. J Neurochem 1997, 68:1135–1141
53. Davis J, Cribbs DH, Cotman CW, Van Nostrand WE: Pathogenic amyloid beta-protein induces apoptosis in cultured human cerebrovascular smooth muscle cells. Amyloid 1999, 6:157–164
54. Harkness KA, Coles A, Pohl U, Xuereb JH, Baron JC, Lennox GG: Rapidly reversible dementia in cerebral amyloid inflammatory vasculopathy. Eur J Neurol 2004, 11:59–62
55. Eng JA, Frosch MP, Choi K, Rebeck GW, Greenberg SM: Clinical manifestations of cerebral amyloid angiopathy-related inflammation. Ann Neurol 2004, 55:250–256
56. Oh U, Gupta R, Krakauer JW, Khandji AG, Chin SS, Elkind MSV: Reversible leukoencephalopathy associated with cerebral amyloid angiopathy. Neurology 2004, 62:494–497